

National Aeronautics and Space Administration (NASA) Astrophysics Data System (ADS).

Appendix B: Gaia DR3 data of asteroseismically modelled *Kepler* γ Dor and SPB stars

We extracted the *Gaia* DR3 time series in the *Gaia* *G*-band for 63 well-known bona fide g-mode pulsators assembled in Aerts et al. (2021). This sample consists of 37 γ Dor and 26 SPB pulsators whose internal structure and evolutionary stage have been modelled asteroseismically using *Kepler* photometric time series that were reduced by Van Reeth et al. (2015) and Pedersen et al. (2021). The *Kepler* light curves typically have a total time base of ~ 1470 d and between some 24 000 and 66 000 data points, with an even sampling time of ~ 30 minutes (Koch et al. 2010). The *Gaia* DR3 epoch photometric data of these g-mode pulsators is sparsely sampled, containing between 34 and 52 data points spread over a time base of between about 910 and 920 d. We re-analysed these *Kepler* light curves in the Fourier domain in the same way as was done for the *Gaia* DR3 *G*-band epoch photometry, using the generalised Lomb-Scargle periodogram (Zechmeister & Kürster 2009), and extracted the two dominant frequencies in the interval $[0, 25] \text{ d}^{-1}$. After derivation of the dominant periodic signal, the second strongest frequency was extracted after prewhitening of the dominant frequency and its harmonics up to fourth order.

Given that the *Kepler* data are almost free of any aliasing, while instrumental effects occur at the level of only a few μmag , we know the two dominant frequencies of these 63 g-mode pulsating dwarfs up to high precision. This allows us to assess the occurrence of the instrumental effects present in the *Gaia* DR3 *G*-band epoch photometry, which occur at mmag level and hence contaminate the pulsational g-mode signal quite severely. Figure B.1 shows a histogram with the 63 pulsators according to their dominant g-mode frequency deduced from the *Kepler* data (in blue). The dominant frequency in the *Gaia* data is indicated by the black hatched histogram and reveals that most of the detected dominant frequencies occur above 6 d^{-1} indicating that they are either aliased frequencies or frequencies of instrumental origin.

The passband of the *Kepler* CCDs is somewhat bluer and narrower than the *Gaia* *G*-band. Moreover, the 63 g-mode pulsators each reveal tens of g modes with accompanying multi-periodic beating in time (Van Reeth et al. 2015; Pedersen et al. 2021). The amplitude of the dominant signal in the *Kepler* and *Gaia* *G*-band are therefore not expected to be equal. Nevertheless, they are of the same order, and so it is meaningful to consider their distributions. This is revealed in Fig. B.2, which shows the dominant frequencies detected in the 126 light curves, in grey for the *Gaia* DR3 *G*-band data and in colour for the *Kepler* data (pink for the 37 γ Dor stars and blue for the 26 SPB stars). It can be seen that the majority of the mode frequencies occurs in the range $[0.2, 3.1] \text{ d}^{-1}$, as is well known for gravito-inertial modes in rotating stars (Aerts et al. 2021). The dominant modes of these 63 well-known g-mode pulsators have amplitudes covering the range $[0.5, 33] \text{ mmag}$, with the majority well below 10 mmag. While several of the dominant frequencies detected in the *Gaia* *G*-band occur in the appropriate frequency range, Figure B.2 clearly shows the presence of peaks at high frequencies, which are either aliased frequencies or periodic instrumental artefacts.

Close inspection of Fig. B.2 reveals that 6 of the 37 γ Dor stars (16%) and 4 of the 26 SPB stars (15%) share the same dominant intrinsic g-mode frequency in their *Kepler*

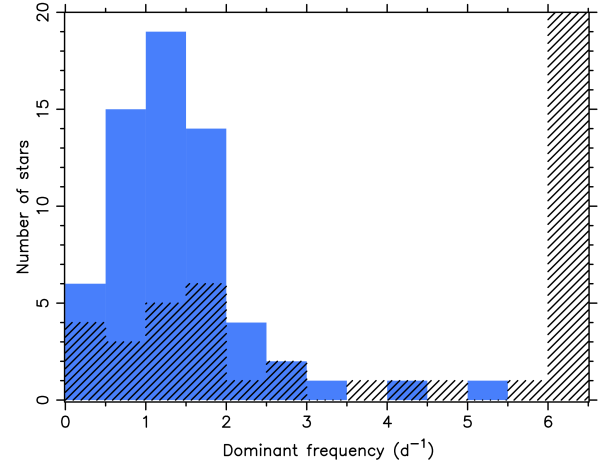


Fig. B.1. Histogram of the dominant frequency in the *Kepler* light curves of 63 asteroseismically modelled g-mode pulsators (blue) compared with the dominant frequency occurring in their *Gaia* DR3 *G*-band epoch photometry (black hatched). For reasons of visibility, the x -axis is cut at 6.5 d^{-1} and the y -axis at 20; 38 of the 63 g-mode pulsators have their *Gaia* data dominated by instrumental effects with dominant frequency above 6 d^{-1} rather than by their g modes.

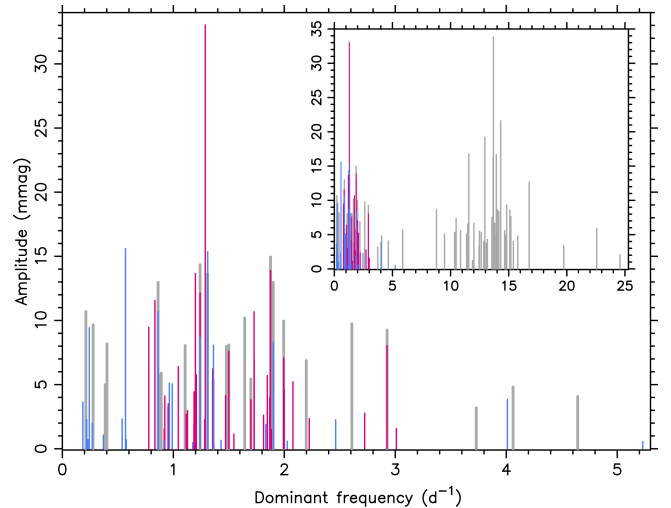


Fig. B.2. Amplitudes of the dominant frequencies in the *Gaia* *G*-band DR3 light curves (grey) and in the *Kepler* light curves of the γ Dor (pink) and SPB (blue) pulsators. The inset shows the entire frequency range, while the main panel focuses on the range of the true dominant g-mode frequencies of the 63 stars.

and *Gaia* *G*-band data. This is illustrated for the γ Dor star KIC 11080103 in Fig. B.3 and for the SPB KIC 4936089 in Fig. B.4. KIC 11080103 has a dominant prograde dipole mode with frequency 1.241393 d^{-1} and amplitude of 12.13 mmag in the *Kepler* band (Van Reeth et al. 2015). The SPB star KIC 4936089, whose periodograms are shown in Fig. B.4, has a dominant g-mode frequency of 0.866263 d^{-1} with an amplitude of 6.26 mmag. Its *Kepler* light curve revealed a period spacing pattern consisting of 13 zonal dipole modes of consecutive radial order. This SPB star ranks number 8 of 26 in terms of dominant mode amplitude, yet the 52 *Gaia* *G*-band data points do allow to pick up the dominant mode, thanks to relatively modest instrumental contamination for this star (Fig. B.4). These two examples show that the amplitude of the dominant frequency peak in the

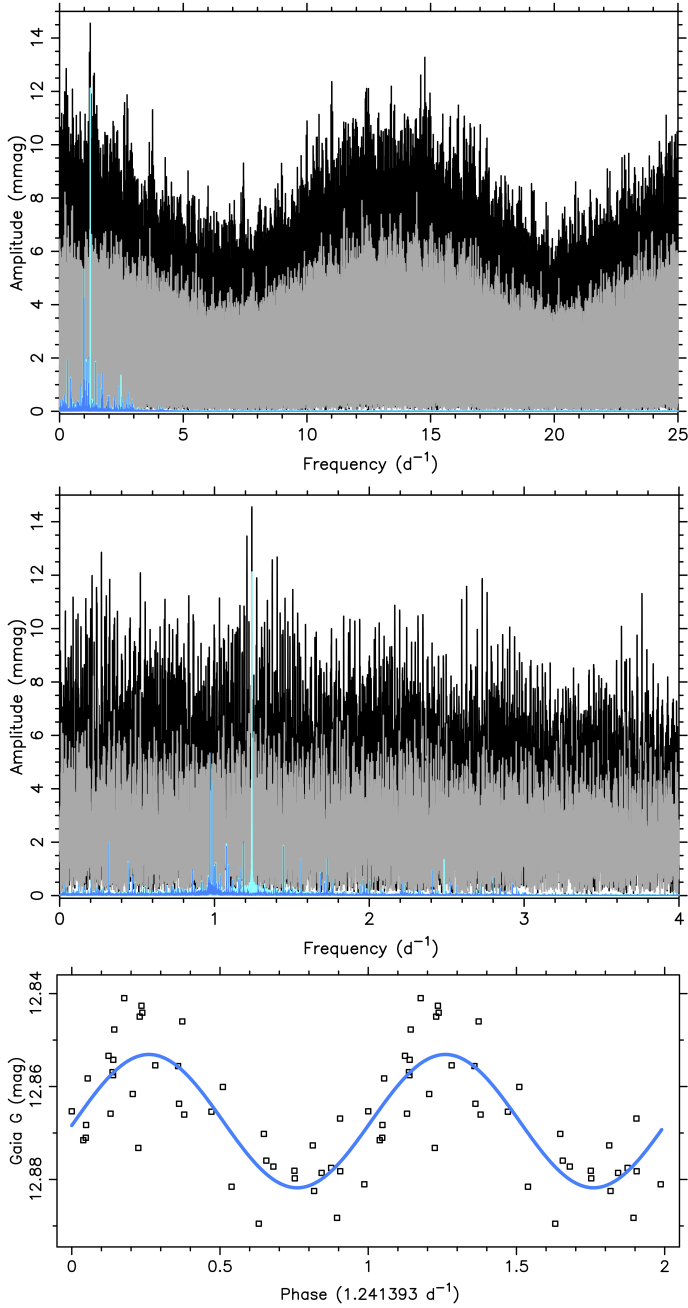


Fig. B.3. Four Lomb-Scargle periodograms (upper: full frequency range; middle; zoomed version) of the γ Dor star KIC 11080103. The black and cyan curves stand for the Gaia DR3 G-band and *Kepler* light curves, respectively. The grey and blue periodograms result from prewhitening the Gaia G and *Kepler* data with the dominant frequency. The lower panel shows the Gaia DR3 G-band data (black squares) folded with the dominant frequency detected in common in both light curves; a harmonic fit with that frequency is overplotted (full blue line). For visibility purposes, the phase is shown for two cycles.

periodogram is not a good criterion to select g-mode pulsators (compare the upper panels of Figs B.3 and B.4).

KIC 11080103 and KIC 4936089 are representative for six of the other cases where *Kepler* and Gaia G-band data lead to the same dominant frequency, with similar morphologies in the periodograms as those shown in Figs B.3 and B.4. It concerns the four γ Dor stars KIC 3448365, KIC 7365537, KIC 7434470, KIC 9480469, with dominant g-mode frequen-

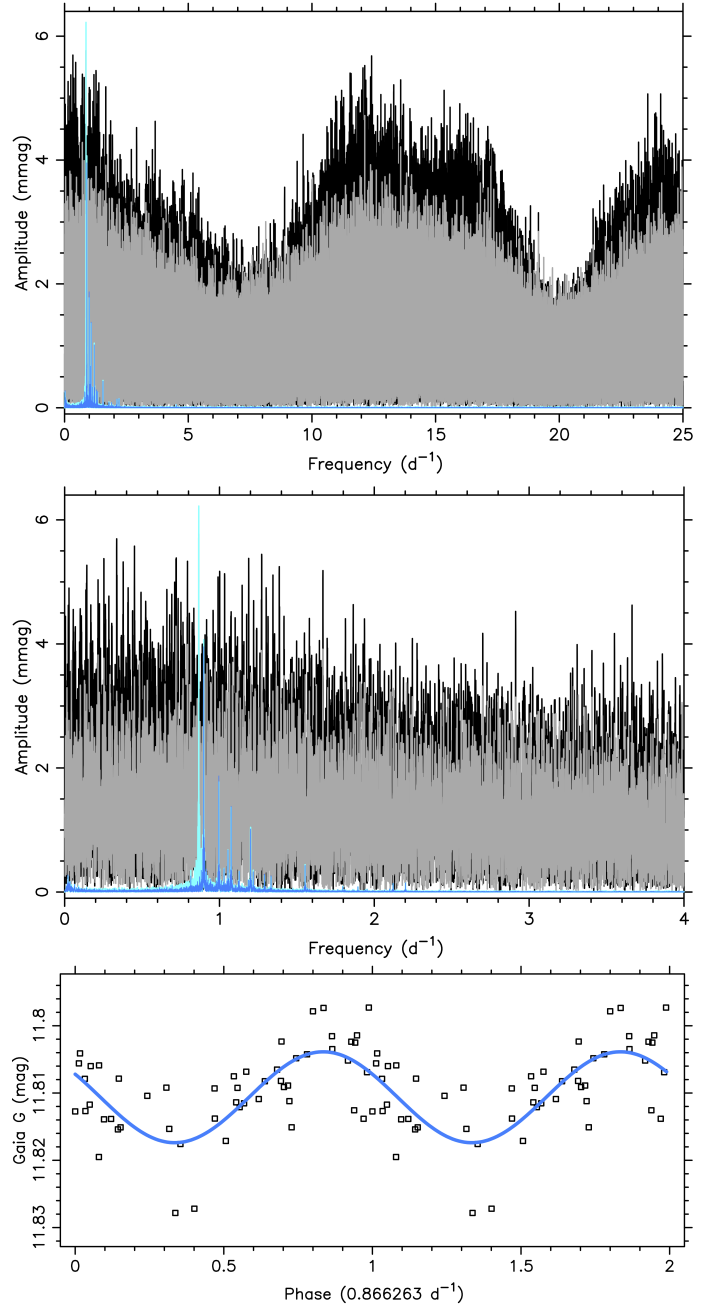


Fig. B.4. Same as Fig. B.3, but for the SPB star KIC 4936089.

cies of 1.500150 d^{-1} , 2.925633 d^{-1} , 1.698729 d^{-1} , 1.994846 d^{-1} , respectively, and the two SPB stars KIC 5941844 and KIC 9020774 with dominant frequencies of 1.309558 d^{-1} and 1.900723 d^{-1} .

For one single γ Dor star, KIC 7023122, and one single SPB star, KIC 7760680, also the second strongest frequencies coincide in the *Kepler* and Gaia G data. The four phase diagrams of these two ‘best cases’ among the g-mode pulsators are shown in Figs B.5 and B.6. These two examples show that, despite the limited number of measurements in the DR3 time series, Gaia’s G-band data already allow us to detect multiperiodic non-radial oscillations at mmag level, albeit it for a very small fraction (3%) of pulsating dwarfs pulsators.

We also checked for all 63 stars if it is meaningful to use the fraction of the variance in the data explained by a harmonic fit

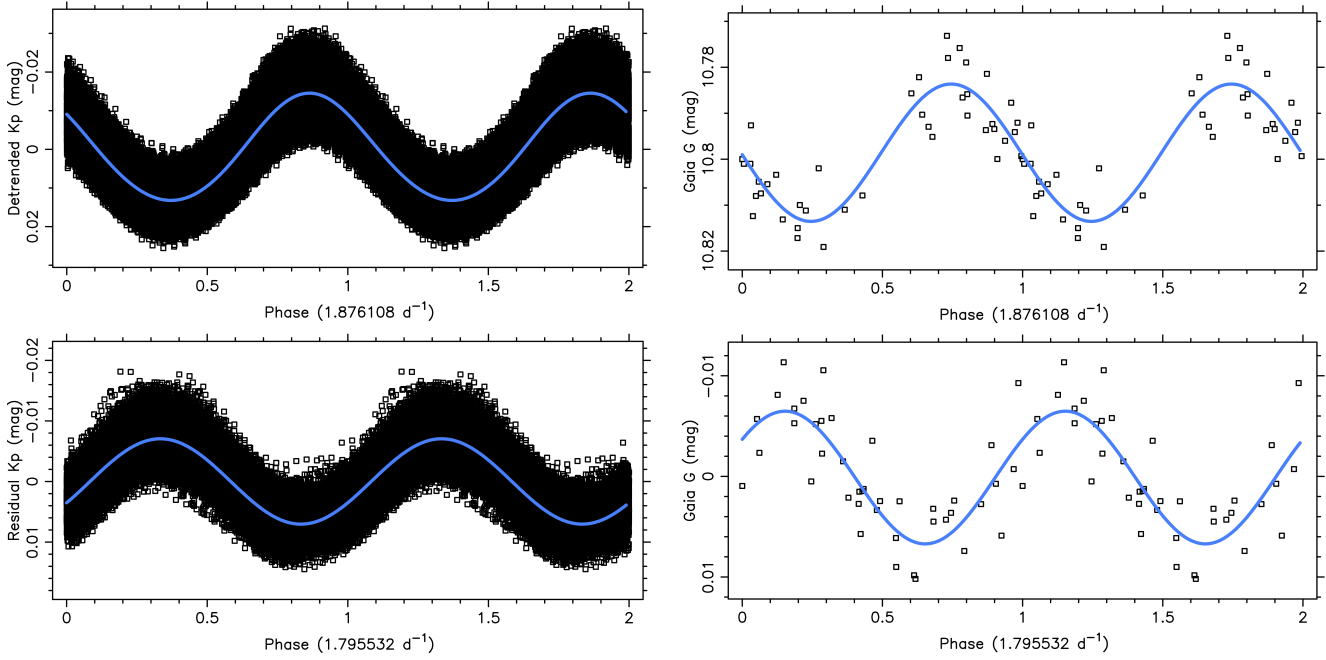


Fig. B.5. Four phase diagrams for the γ Dor pulsator KIC 7023122 whose two dominant g-mode frequencies (as listed in the legend of the x -axes) occur consistently in the periodograms of the Gaia DR3 G-band and *Kepler* photometry. The data are shown as black squares and the best harmonic fits for the fixed frequencies as blue lines. For visibility purposes, the phases are shown for two cycles.

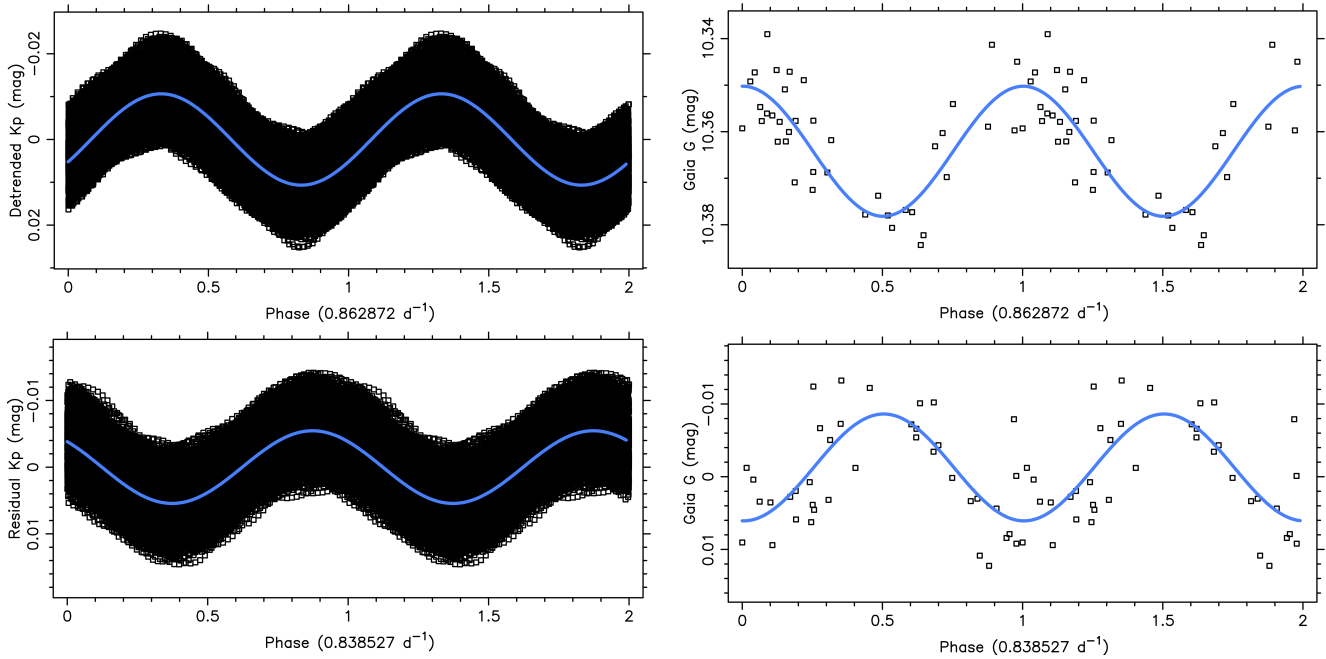


Fig. B.6. Same as Fig. B.5 but for the SPB star KIC 7760680.

with the dominant frequency as a selection criterion to distinguish intrinsic g-mode frequencies from instrumental frequencies. We found this not to be feasible, as this merit function attains similar values for instrumental and intrinsic frequencies. The corresponding phase diagrams also do not allow to distinguish between intrinsic and aliased/instrumental frequencies in a meaningful way. This is illustrated in Fig. B.7 for the largest-amplitude γ Dor pulsator of the sample. Figure B.7 shows two

phase diagrams based on the 40 Gaia DR3 G-band data points: one based on the ‘true’ intrinsic dominant g-mode frequency reducing the variance by 47% and another one using the dominant frequency in the data themselves, which is either aliased or of instrumental origin. The latter frequency reduces the variance by 58%. Hence the variance reduction cannot be used as a criterion to distinguish between instrumental and true frequencies in *Gaia*’s DR3 time series.

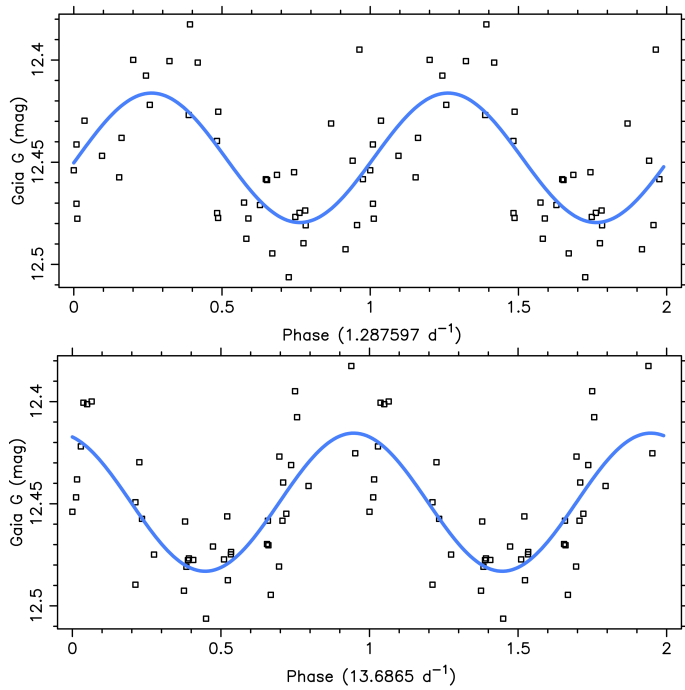


Fig. B.7. Two phase diagrams for the largest-amplitude g-mode pulsator in the γ Dor sample. The upper graph is phase-folded with the true dominant g-mode frequency derived from *Kepler* data; its fit leads to a variance reduction in the Gaia DR3 G-band data of 47%. The lower graph is phase-folded with the dominant frequency in the data, which is of instrumental origin and reduces the variance with 58%.